NMR Study of the Conformation of Galactocerebroside in Bilayers and Solution: Galactose Reorientation during the Metastable−Stable Gel Transition†

Karol S. Bruzik*

Department of Medicinal Chemistry and Pharmacognosy (m/c 781), University of Illinois at Chicago, Chicago, Illinois 60612

Per-Georg Nyholm

Structural Chemistry, Department of Medical Biochemistry and MEDNET Laboratory, Göteborg University, Göteborg, Sweden

Received August 28, 1996; Revised Manuscript Received November 12, 1996⊗

ABSTRACT: Conformations of two types of bovine brain cerebroside containing normal and α-hydroxy-fatty acids (NFA-CER and HFA-CER, respectively) in solution and in bilayers were investigated using ^{1}H and ^{13}C NMR in solution and in the solid state. The analysis of vicinal ^{1}H−^{1}H coupling constants and NOE measurements in solution indicated that in both cerebrosides the predominant conformation about the O1−C1, C1−C2, and C2−C3 bonds is ap/−sc/ap, respectively. The remarkable similarity in the ^{13}C NMR chemical shifts in solution and in hydrated liquid-crystalline bilayers indicated that both cerebrosides in bilayers assume conformations essentially identical to those in solution. The obtained ^{13}C NMR spectra in solution were used as a reference for comparison with the variable-temperature ^{13}C CP-MAS NMR spectra in the metastable and stable gel phases. The lack of chemical shift changes of polar carbon atoms upon cooling the HFA-CER bilayers below the T_m strongly suggests that the liquid-crystalline−metastable gel transition is not associated with a conformational change of the head group. The observed line broadening can be interpreted in terms of the hydrocarbon chain crystallization and slow dynamics of the head group in the metastable phase. On the other hand, the relaxation of the metastable gel phase of HFA-CER caused profound changes in the ^{13}C spectra, primarily of the signals of the galactose C1, the ceramide C2, C4, and C5, and the carbonyl group. These changes are interpreted using the known dependence of the chemical shifts of anomeric carbon on the conformation about the O1−C1 bond to suggest that the gel phase relaxation involves a significant reorientation of the galactose moiety caused by a change in the rotation of the O1−C1 bond from the ap to −sc conformer. Similar changes of chemical shifts were observed in the case of NFA-CER during the transition from the liquid-crystalline phase to the stable gel phase.

Cerebrosides (CER)[1] are the simplest members of the glycosphingolipid (GSL) family of relatively minor, but functionally important, constituents of cell membranes in animal and plant tissues (Hakomori, 1995). These lipid molecules present their mono- or oligosaccharide residues into the extracellular space, exposing them to interactions with glycolipid head groups of other cells, antibodies, bacterial toxins, and viral envelope proteins. Glycosphingolipids are therefore important in cell adhesion, in mediating cellular immunity, in determining blood groups, and as tumor antigens. Recently, synthetic analogs of galactosylceramides have been shown to possess immunostimulatory and antitumor activity (Motoki et al., 1995), and the sulfated analogs have been shown to be active against HIV-1 (Yoshida et al., 1995), most likely by binding to the viral envelope protein gp120 (McCalarney et al., 1994). Because the function of GSL involves recognition processes, the steric presentation of the saccharide moiety at the bilayer surface is of paramount importance. These aspects of GSL structure have been recently investigated using computational methods (Nyholm & Pascher, 1993; Nyholm et al., 1989, 1990). Conformational properties of the related diacylglycerogly-cosides have been studied by a combination of molecular modeling and solid-state NMR (Howard & Prestegard, 1995).

In contrast to glycerolipids which form a variety of phases with different molecular architectures, the hydrated sphingolipids form only three main supramolecular structures: the lamellar liquid-crystalline phase (L_α), the metastable gel phase obtained by cooling from temperatures above the main transition (T_m), and the stable gel phase obtained by relaxation of the metastable phase (Curatolo, 1982; Ruocco et al., 1981; Curatolo & Jungalwala, 1985; Ruocco & Shipley, 1986; Reed & Shipley, 1987; Haas & Shipley, 1995; Koynova & Caffrey, 1995). The two major types of galactocerebrosides, the nonhydroxy-fatty acid-containing cerebrosides (NFA-CER, Figure 1) and the hydroxy-fatty acid-containing cerebrosides (HFA-CER), display different phase properties (Curatolo, 1982; Curatolo & Jungalwala, 1985). The bilayers of NFA-CER readily form a rigid stable gel phase upon cooling the liquid-crystalline phase (L_α). This stable gel phase is characterized by a high main transition enthalpy (Curatolo, 1982; Curatolo & Jungalwala, 1985; Haas & Shipley, 1995). In contrast, the L_α phase of HFA-CER

† This work was supported by Research Grant GM 30327 from the National Institutes of Health (to M.-D. Tsai), and by the Department of Medicinal Chemistry and Pharmacognosy of the University of Illinois at Chicago.

⊗ Abstract published in *Advance ACS Abstracts,* January 1, 1997.

[1] Abbreviations: CP, cross-polarization; GSL, glycosphingolipids; HFA-CER, hydroxy-fatty acid-containing cerebroside; MAS, magic angle spinning; NFA-CER, nonhydroxy-fatty acid-containing cerebroside; NOE, nuclear Overhauser enhancement; SPM, sphingomyelin.

S0006-2960(96)02204-0 CCC: $14.00

was shown to undergo a very slow conversion to the stable gel phase, with initial transition to a metastable gel phase which displayed a typical value of ΔH_m (Curatolo, 1982; Curatolo & Jungalwala, 1985). Studies of both phases by X-ray diffraction (Ruocco et al., 1981; Ruocco & Shipley, 1986; Reed & Shipley, 1987; Haas & Shipley, 1995; Norberg et al., 1996) indicated that the metastable−stable gel phase transition involves a change from the layer-perpendicular to the layer-tilted arrangement of hydrocarbon chains. The relaxation of the more expanded metastable phase into the more tightly packed stable gel phase is probably accompanied by head group dehydration (Ruocco et al., 1981), and a change of the available area per head group. These changes are likely to alter the orientation of the galactose head group with respect to the bilayer surface. The ^{2}H NMR study of the liquid-crystalline phase of glucocerebroside showed that the hexose ring is oriented perpendicularly to the bilayer (Skarjune & Oldfield, 1982), whereas the X-ray crystal studies of cerebrosides (Pascher & Sundell, 1977; Nyholm et al., 1990) suggested that conformations with a layer-tilted orientation of the galactose residue are also possible in more condensed phases.

The differences in structural and dynamic properties of lipid molecules in various bilayer phases can be explored using variable-temperature ^{13}C CP-MAS NMR (Li et al., 1993; de Meulendijcks et al., 1989; Forbes et al., 1988a,b; Bruzik et al., 1988b, 1990). This technique is particularly well suited for simultaneous observation of multiple sites in the molecule, to afford highly coherent integrated information. In the cases where chemical shifts of ^{13}C signals can be interpreted in terms of specific conformations, monitoring changes in ^{13}C CP-MAS spectra can afford a detailed description of lipid phase transitions at a molecular level. In this work, we report on the application of this technique to study conformational changes occurring during the metastable−stable gel transition of cerebrosides. The conformations of cerebrosides in solution were determined by a classical approach using a ^{1}H−^{1}H coupling constant and NOE data. For the particular set of conformations of cerebrosides populated in the solution state, as observed by ^{1}H NMR, reference ^{13}C NMR spectra were obtained. These spectra were used as a starting point for interpretation of changes in chemical shifts in ^{13}C CP-MAS spectra of bilayers, induced by lipid phase transitions.

MATERIALS AND METHODS

NFA-CER and HFA-CER were obtained from the total lipid extract of bovine brain and separated by silica gel chromatography using chloroform−methanol (10:1) as an eluting solvent. Cerebrosides thus obtained were further purified by acetone precipitation from chloroform−methanol solution. Consistent with the typical fatty acid composition of sphingolipids (O'Brien & Rouser, 1964), the ^{1}H and ^{13}C NMR spectra indicated that NFA-CER contains more unsaturated fatty acids than HFA-CER (0.50 vs 0.26 double bond per fatty acid chain, respectively). The permethylated sample of cerebroside was obtained as described earlier (Nyholm et al., 1990). ^{1}H NMR spectra were recorded with Bruker AM-500, AC-250, AC-200, and MSL-300 spectrometers, and chemical shifts were indirectly referenced to TMS. ^{13}C NMR spectra in solution were obtained for CD_3OD−$CDCl_3$ (5:1, v/v) solutions unless otherwise indicated. The choice of the solvent was dictated by the compromise between the line width and the specimen solubility. Solvents with higher content of chloroform gave less resolved spectra, resulting from lipid aggregation in media of low dielectric constant. Based on the small line width observed (ca. 0.5 Hz) in methanol−chloroform (up to 20% chloroform), it is believed that in such solutions cerebroside molecules exist as monomers. ^{13}C CP-MAS spectra were obtained with Bruker MSL-300 spectrometer using cerebroside samples prepared as follows: Samples of NFA-CER and HFA-CER (50 mg) were hydrated by adding an equal amount of water (w/w), and the mixture was homogenized by passing it through a narrow constriction in the glass ampule by centrifugation. The resulting semi-solid was loaded into a special glass ampule (Wilmad) also by centrifugation. The top of the ampule was sealed with an epoxy resin, and the ampule was inserted inside a 7 mm (o.d.) zirconium oxide MAS rotor. Stable rotation rates of 4 kHz could be routinely obtained with this assembly. The size of samples thus prepared was limited to approximately 100 μL. The whole assembly was kept at 353 K for 1 h, prior to measurement, for the purpose of annealing. The annealed sample was quickly transferred to the preheated NMR probe in such a manner as to avoid a drop in the sample temperature. Chemical shifts in CP-MAS spectra were indirectly referenced to the glycine carbonyl carbon (176.06 ppm) using the standard reference numbers determined with the glycine standard prior to each session. During each measurement session, the magnet shim parameters obtained for the standard glycine sample were kept constant to avoid shim-induced field change. The CP-MAS spectra were obtained using a cross-polarization pulse sequence with a 4.5 μs 90° ^{1}H pulse, a single 1 ms contact time, a 50 ms acquisition−decoupling time, and a 4 s relaxation delay.

Table 1: ^{1}H−^{1}H Coupling Constants for NFA-CER and HFA-CER in CD_3OD−$CDCl_3$ at 300 K and DMSO-d_6

	NFA-CER		HFA-CER	
protons	$CDCl_3$−CD_3OD	DMSO-d_6	$CDCl_3$−CD_3OD	DMSO-d_6
1_a−1_b	10.3	10.5	10.3	10.5
1_a−2	4.6	5.1	5.5	5.7
1_b−2	3.3	3.6	3.5	3.7
2−3	7.8	7.6	7.5	6.9
3−4	7.7	7.4	7.4	7.9
4−5	15.4	15.3	15.3	15.4
4−6	1.5	nd[a]	1.3	1.4
5−6	6.7	6.8	6.7	6.7
1′−2′	7.6	7.6	7.5	7.5
2′−3′	9.7	9.6	nd	nd
3′−4′	3.3	3.3	3.3	3.3
4′−5′	1.1	1.0	1.1	1.1
5′−6′	7.0, 5.2	6.7, 5.3	7.0, 5.1	6.8, 5.1
6′−6′	11.3	11.4	nd	11.4
2″−3″	7.6	7.6	3.6, 7.7	4.1, 7.8

[a] nd, not determined.

Conformation of Cerebrosides in Solution

^{1}H NMR of HFA- and NFA-CER. The vicinal coupling constants shown in Table 1 were used to calculate molar fractions of staggered conformers about θ_1 (C1−C2) and θ_3 (C2−C3) angles (Figures 1 and 2). Because of the uncertainty of the assignment of the diastereotopic protons $H1_a$ (lower field) and $H1_b$ (higher field) to the *pro-S* and *pro-R*

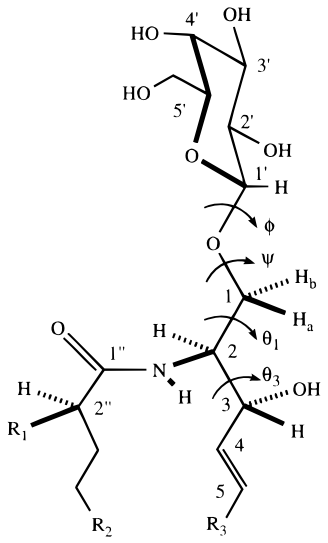

NFA-CER, R_1 = H, R_2 = C_nH_{2n-1}, R_3 = C_nH_{2n+1}

HFA-CER, R_1 = OH, R_2 = C_nH_{2n-1}, R_3 = C_nH_{2n+1}

ϕ: O5'-C1'-O1-C1

ψ: C1'-O1-C1-C2

θ_1: O1-C1-C2-C3

θ_3: C1-C2-C3-C4

FIGURE 1: Structure of NFA-CER and HFA-CER, showing atom numbering and the nomenclature of the torsional angles discussed in this work. The nomenclature of conformers is according to Klyne and Prelog (1960).

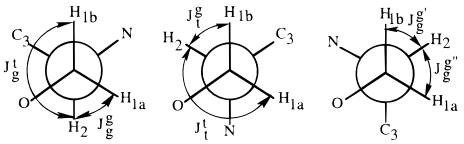

Rotamer (θ_1)	+sc	ap	-sc
NFA-CER	0.04 (0.25)	0.31 (0.12)	0.65 (0.63)
HFA-CER	0.04 (0.35)	0.41 (0.12)	0.55 (0.53)

FIGURE 2: Projections and populations of the staggered conformers (θ_1) about the C1−C2 bond of sphingosine in NFA-CER and HFA-CER. The corresponding component coupling constants were calculated using the seven-parameter equation of Altona (Haasnot et al., 1979), and are the same as used in the previous work (Bruzik, 1988b); J^t_g 10.8 Hz, J^g_g 3.9 Hz, J^g_t 4.5 Hz, J^t_t 10.8 Hz, $J^{g'}_g$ 2.2 Hz, $J^{g''}_g$ 1.6 Hz. The populations were calculated using coupling constants listed in Table 1 and the stereochemical assignments H_{1a} = *pro-S* and H_{1b} = *pro-R* as shown in the diagrams. The numbers given in parentheses are conformer populations calculated using the reverse assignment.

positions, two sets of molar fractions of conformers about θ_1 can be derived from the coupling constants. The reversal of the assignment has a significant effect only on the relative ratio of the minor θ_1 = +sc and θ_1 = ap conformers, while the population of the major −sc conformer remains relatively unaffected. In essence, the presence of the hydroxyl function at the 2-position of the fatty acid in HFA-CER decreases only slightly the population of the θ_1 = −sc rotamer as compared to NFA-CER. The conformation about the C2−C3 bond (θ_3) is mainly ap (ca. 70%, as inferred from the magnitude of H2−H3 coupling), and thus both θ_1 and θ_3 rotamer distributions resemble the ones of sphingomyelin in solution (Bruzik, 1988b).

The distance between the H1′ and the $H1_a$ and $H1_b$ protons is affected by the conformations about C1′−O1 (ϕ) and O1−C1 (ψ), and can be determined by measuring the 1D- and 2D-NOE effects, using an internal reference NOE for the $H1_a$−$H1_b$ pair of protons separated by a known intramolecular distance (1.73 Å). The corresponding partial NOESY spectra of HFA-CER and NFA-CER are shown in Figure 3A and Figure 3B, respectively. In both NOESY spectra, the strong cross-relaxation peaks are observed between H1′ and $H1_b$, while the interactions between H1′ and $H1_a$ are much weaker. The observation of the strong and equally intense cross-peaks between H2 and $H1_a$ and $H1_b$ is consistent with the predominant θ_1 = −sc conformation inferred from the analysis of the coupling constants. On the other hand, the absence of the H2−H3 and H3−$H1_b$ cross-peaks is also consistent with the −sc/ap combination of θ_1 and θ_3 angles.

The 1D-NOE effects measured from the NOE difference spectra of NFA-CER obtained by irradiation of the H1′ proton (Figure 4) were 0.06 (H1′−$H1_b$) and 0.25 (a sum of H1′−H3′, H1′−H2′, and H1′−H5′ interactions). Similar values of 0.04 (H1′−$H1_b$) and 0.23 (H1′−H3′, H1′−H2′, and H1′−H5′) were obtained for HFA-CER (not shown). As an internal calibration, the NOE between $H1_a$ and $H1_b$ of NFA-CER was measured (0.23, Figure 4B). In the case of HFA-CER, such calibration was not possible due to an overlap of $H1_b$ and H6′ signals, the closeness of the resonances of H1′ and $H1_a$, and an overlap of $H1_a$ and H3 signals.

Temperature Dependence of Chemical Shifts of Exchangeable Protons. Assignments of all exchangeable protons by COSY spectra in DMSO-d_6 (not shown) through their couplings to C−H protons were found in full agreement with those previously reported (Dabrowski et al., 1980). The chemical shifts of all OH protons displayed very similar temperature dependence, suggesting that at least in DMSO these protons were not involved to a significant degree in intramolecular hydrogen bonding. In contrast, the amide proton in HFA-CER displayed only half as high temperature dependence as the analogous proton in NFA-CER (Figure 5), indicating that this proton is involved in hydrogen bonding, most likely with the 2″-OH group of the α-hydroxy-fatty acid. This conclusion is consistent with the downfield chemical shift of the 2″-OH signal (5.4 ppm at 350 K, ca. 1.0 ppm lower than typical non-hydrogen-bonded OH signals).

^{13}C NMR in Solution. Although assignments of ^{13}C resonances for cerebrosides and other sphingolipids have been previously published (Dabrowski et al., 1980; Koerner et al., 1979; Sillerud et al., 1978; Harris & Thornton, 1978; Sarmientos et al., 1985; Forbes et al., 1988a,b; Bruzik, 1988a), the detailed analysis of ^{13}C shifts performed in this work (see Discussion) required confirmation of their assignments. To our surprise, we have found previous assignments to be in error with respect to the sphingosine C4 and C5 signals. Shown in Figure 6 are ^1H−^{13}C HETCOR spectra of NFA-CER (A) and HFA-CER (B) in CD_3OD−$CDCl_3$ solution. The lower field olefinic ^{13}C signal at 134 ppm is clearly correlated with the olefinic proton at 5.69 ppm, and the higher field signal at 129 ppm with the proton at 5.45 ppm. The additional cross-peak in this range of chemical shifts arises from the *cis*-olefinic double bond of the fatty acid (shown as a triplet in the ^1H projection). The coupling

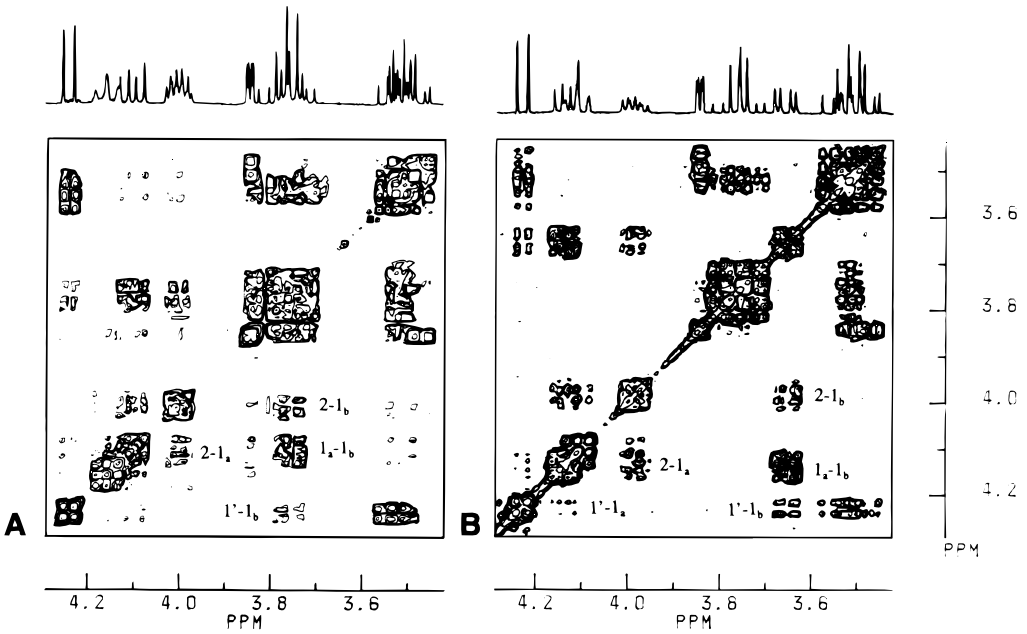

FIGURE 3: 300 MHz NOESY spectra of HFA-CER (A) and NFA-CER (B) in $CD_3OD-CDCl_3$ (5:1 v/v) obtained at 313 K with 500 ms mixing time.

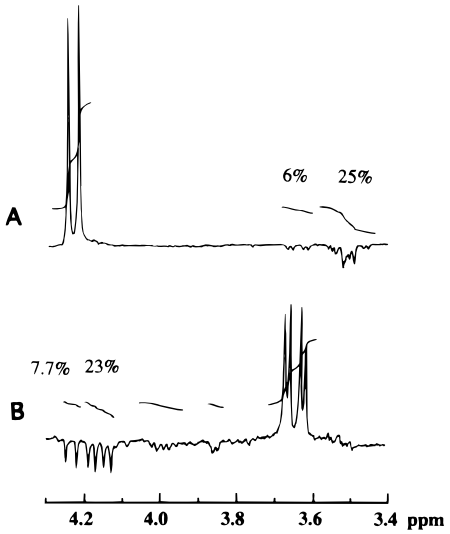

FIGURE 4: NOE difference spectra of NFA-CER in $CD_3OD-CDCl_3$ (5:1 v/v) at 313 K. (A) Irradiation at the position of the anomeric proton (4.22 ppm). (B) Irradiation at the position of the $H1_b$ proton (3.65 ppm).

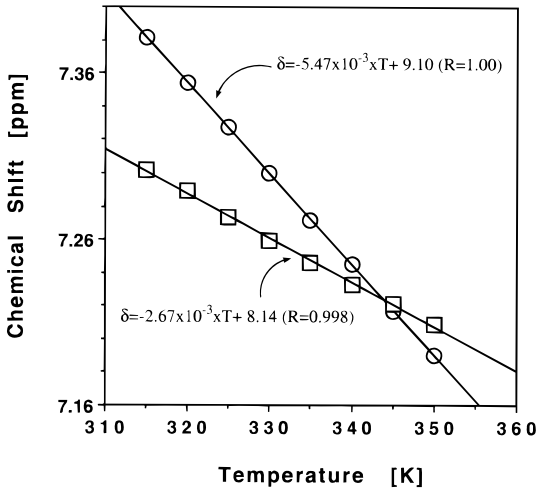

FIGURE 5: Temperature dependence of the chemical shifts of NH protons in NFA-CER (circles) and HFA-CER (squares) in DMSO-d_6 solution.

pattern of the proton signals and $^1H-^1H$ COSY spectra (not shown) clearly indicated assignment of the lower field proton as H5, and the higher field one as H4 as previously reported (Bruzik, 1988a; Dabrowski et al., 1980, 1988a,b). The previous ^{13}C assignment (Sillerud et al., 1978) was based on the chemical shift additivity rules, which apparently do not hold here. The positions of C4 and C5 resonances are strongly affected by the solvent, and are almost identical in the DMSO solution (Dabrowski et al., 1980). It is expected that this ^{13}C signal assignment should also hold for other sphingoids. The ^{13}C chemical shifts of NFA-CER and HFA-CER in solution and liquid-crystalline bilayers and their assignments are listed in Table 2.

Comparison of ^{13}C NMR Spectra in Solution and Liquid-Crystalline Bilayers. Inspection of Table 2 shows a remarkable similarity of chemical shifts in solution and liquid-crystalline bilayers with most of the chemical shifts differing by less than 1 ppm. Furthermore, it should be noted that all signals in the bilayers are slightly shifted downfield (ca. 0.2−0.3 ppm) as compared to the solution spectra, reflecting probably the mismatch between the referencing systems used for solution and bilayers. If, instead of using TMS and the glycine carbonyl group, the terminal methyl group of the hydrocarbon chain is used as an internal reference in both physical states, most of the differences are within 0.5 ppm, except for a few carbon atoms listed below. The most notable differences observed for NFA-CER are for the carbonyl group carbon atom (0.7 ppm), sphingosine C1 (0.7 ppm), and C2 (1.0 ppm). In the case of HFA-CER, the largest differences were registered for the carbonyl group (1.4 ppm), C1 (1.0 ppm), C2 (0.4 ppm), and C3 (0.7 ppm). The significant downfield shift of the carbonyl group for both cerebrosides in the bilayers could be explained by its involvement in hydrogen bonding with water molecules in the hydrated liquid-crystalline state. The other differences could be due to slight changes in conformational equilibria about θ_1 and θ_3 angles between the solution and bilayers. These differences are, however, very small as compared to

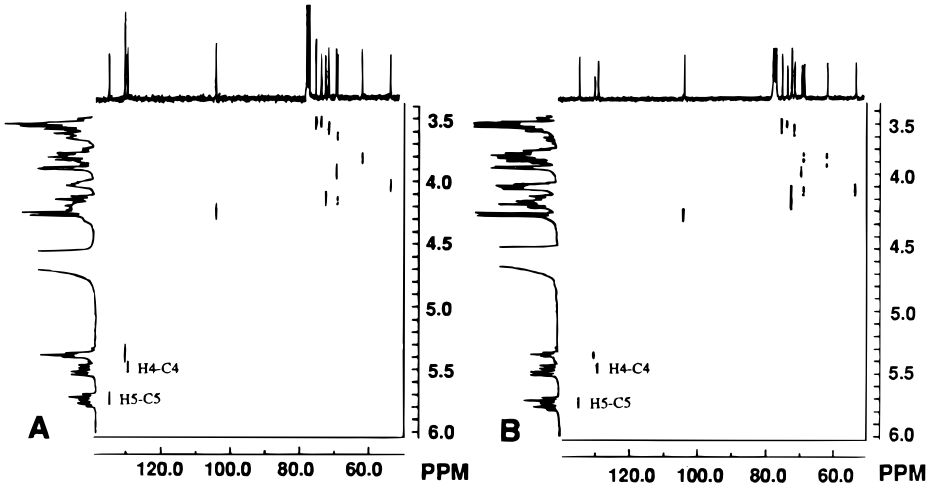

FIGURE 6: 300 MHz $^1H-^{13}C$ HETCOR spectra of NFA-CER (A) and HFA-CER (B) showing H4−C4 and H5−C5 correlations.

Table 2: ^{13}C NMR Chemical Shifts of NFA-CER and HFA-CER in $CD_3OD-CDCl_3$ (5:1 v/v) Solution and in Hydrated Bilayers[a]

carbon atom	NFA-CER			HFA-CER		
	CD_3OD	bilayers	$\Delta\delta$	CD_3OD	bilayers	$\Delta\delta$
C=O	174.3	175.0	+0.7	175.0	176.4	+1.4
C5	134.0	134.1	+0.1	134.1	134.6	+0.5
C4	128.8	129.7	+0.9	128.6	129.9	+1.3
C1′	103.5	103.8	+0.3	103.5	103.7	+0.2
C5′	74.7	75.5	+0.8	74.8	75.5	+0.7
C3′	73.2	73.7	+0.5	73.3	73.6	+0.3
C3	72.0	72.0	0.0	72.0	72.7	+0.7
C2′	71.1	71.5	+0.4	71.1	71.5	+0.4
C4′	68.9	69.8	+0.9	69.1	69.6	+0.5
C1	68.5	69.2	+0.7	68.3	69.3	+1.0
C6′	61.4	61.6	+0.2	61.6	61.6	0.0
C2	53.2	54.2	+1.0	53.2	53.6	+0.4
C2″	36.3	36.9	+0.6	72.0	72.0	0.0
C6	32.1	33.0	+0.9	32.1		
$C_{\omega-2}$	31.7	32.3	0.6	31.7		
$(CH_2)_n$	29.5−29.1	30.4		30.4	29.1	
C3″	27.0	27.4	+0.4	34.3		
$C_{\omega-1}$	22.1	22.8	+0.7	22.4	22.8	+0.4
C_ω	13.7	14.0	+0.3	13.7	13.9	+0.2

[a] Chemical shifts in solution were referenced to TMS, and those in bilayers to the carbonyl carbon of the glycine standard.

5−10 ppm differences (Saito, 1986) that should be observed if major changes in conformation occurred. Most importantly, the position of the C1′ resonance remained almost unaffected (0.3 ppm for NFA-CER and 0.2 ppm for HFA-CER) by the physical state of cerebroside, suggesting that no significant changes in ϕ and ψ angles occurred (see Discussion).

^{13}C CP-MAS NMR Spectra of Hydrated Bilayers

^{13}C CP-MAS spectra of the samples of hydrated bilayers of NFA-CER and HFA-CER recorded at various temperatures, and with different thermal history prior to measurements, are shown in Figures 7 and 8, respectively. Five regions of resonances can be distinguished: those arising from the carbonyl group, Δ4-double bond, anomeric, hydroxylated, and the hydrocarbon carbons. A severe signal overlap in the range of hydroxylated carbons (65−80 ppm) including C2′−C5′ carbons of galactose, C3 and C1 of sphingosine, and C2″ of HFA-CER limits our spectral analysis to signals arising from the carbonyl, C5, C4, C1′, C6′, C2, and the bulk hydrocarbon carbon atoms.

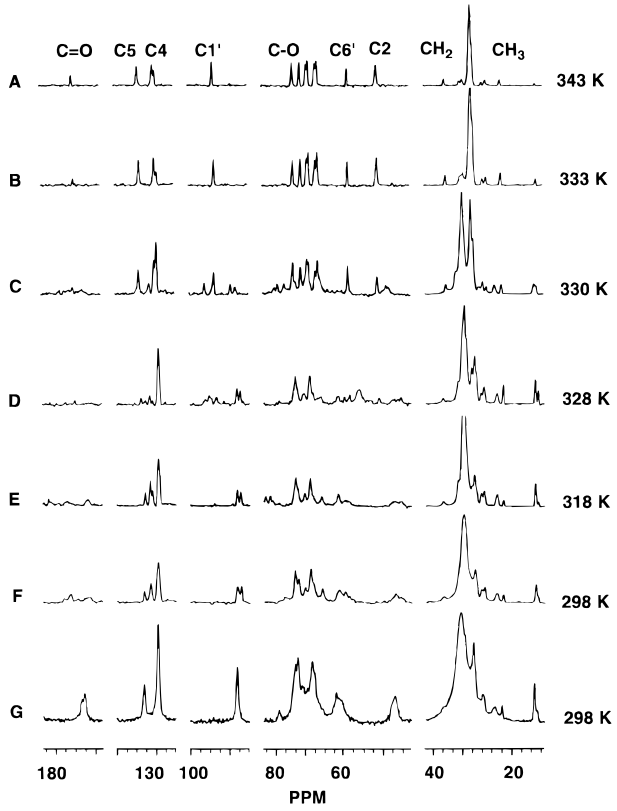

FIGURE 7: ^{13}C CP-MAS NMR spectra of NFA-CER at indicated temperatures. (A) Hydrated sample was annealed at 353 K and quickly brought to 343 K; spectra B−F were acquired sequentially (B−F sequence) by the stepwise lowering of the temperature of the probehead; (G) anhydrous NFA-CER obtained by precipitation with acetone. Spectra consist of 4000−12 000 scans required to achieve the necessary S/N ratio. The FID were transformed using Gaussian apodization with LB = −20 and GB = 0.2−0.5 for resolution enhancement. The intensity of the rightmost fragment of each spectrum was scaled down 3-fold as compared to other parts.

Behavior of NFA-CER. Cooling the sample from 343 K (above T_m) to 333 K (Figure 7A,B) had only the intensity-lowering effect on the carbonyl signal. Further decrease in the temperature to 330 K (Figure 7C) brought about emergence of the resonance at 32.9 ppm, in addition to the existing signal at 30.0 ppm, suggesting the onset of hydrocarbon crystallization. The coexistence of the liquid and solid domains resulted in splitting of numerous resonances

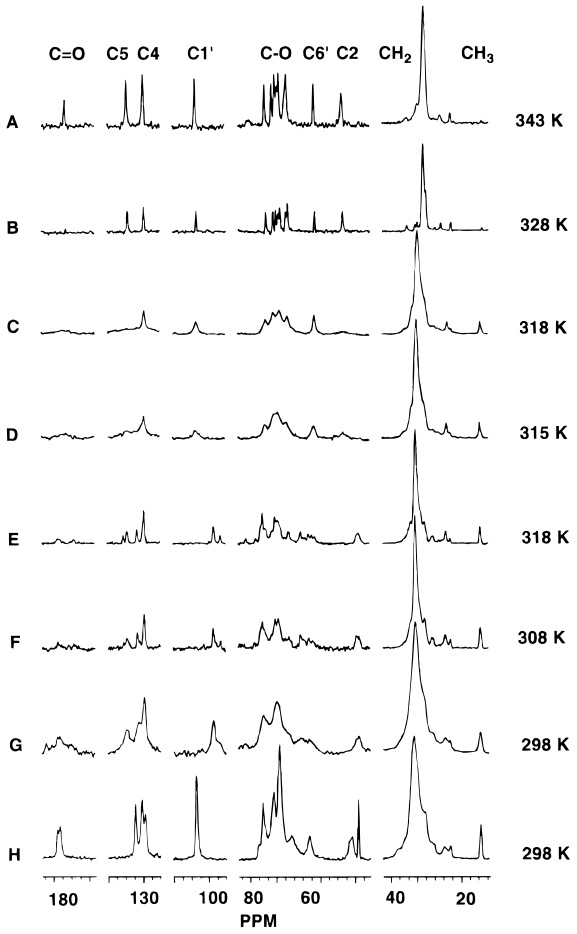

FIGURE 8: ^{13}C CP-MAS NMR spectra of HFA-CER at indicated temperatures. (B−D) Samples were annealed at 353 K and rapidly cooled down to the temperature of measurement by inserting into the probehead with the preset temperature; (E−G) the sample was annealed at 353 K and then incubated at 295 K for 8 h before inserting it into the probehead with the preset temperature; (H) anhydrous HFA-CER obtained by acetone precipitation. The spectra were accumulated and transformed analogously to those in Figure 7.

in the spectrum. Most interestingly, the signal of the anomeric carbon was split into the set of four signals at 106.3, 103.8, 99.6, and 98.4 ppm. The two high-field signals were preserved throughout further bilayer crystallization; therefore, they represent two inequivalent molecules in the fully relaxed crystalline gel state. The signal at 106.3 ppm disappeared on further cooling (e.g., Figure 7E); therefore, it likely represents an intermediate in the transition between the two states. At 330 K (Figure 7C), the C2 carbon gave rise to a new signal at 51.7 ppm (1.5 ppm shift), which was also preserved in the fully relaxed state (Figure 7E,F). At 328 K (Figure 7D), the new peaks increased their intensity, and only very little of the high-temperature signal set remained. In addition, the C6′ signal acquired a very complicated pattern with several lines extending from 66 to 56 ppm. The C1′ carbon gave rise to as many as five different signals. Further cooling to 318 K (Figure 7E) caused a simplification of the spectrum; however, most lines remained duplicated with roughly equal intensities of the doublet components (C═O, 177.1, 172.0; C1′, 98.5, 97.5; C6′, 64.4, 62.8; C2, 50.5, 49.0). The C4 and C5 signals seemed to be also doubled, but their site-specific assignment is uncertain. Further decrease in temperature to 298 K (Figure 7F) caused mainly line broadening without major chemical shift changes. The anhydrous lipid displayed a very similar spectrum (Figure 7G) to that of the relaxed hydrated lipid at 298 K, except that only one signal for every carbon atom was observed. The chemical shifts of C1′ signals closely matched one of the components in the hydrated lipid at 298 K.

Behavior of HFA-CER. The ^{13}C NMR spectra of this lipid were clearly dependent on the thermal history of the lipid sample (Figure 8), which is in agreement with the slow rate of the metastable−stable gel phase transition (Curatolo, 1982; Curatolo & Jungalwala, 1985). Thus, these spectra showed pronounced differences depending on whether the sample was quenched from the liquid−crystalline phase by rapid cooling, or if the sample was incubated at low temperature for several hours prior to acquiring ^{13}C NMR spectra. Cooling the sample from 343 to 328 K (Figure 8A,B) had only an effect on the intensity of the carbonyl signal. In the sample further cooled to 318 K (Figure 8C), the only well-defined signals were those arising from the galactose moiety and the hydrocarbon chains. The carbon atoms of the polar part of sphingosine gave very broad, almost unobservable signals. The broad nature of the ceramide resonances in the C1−C5 region results most likely from the dynamic equilibria affecting this part of the molecule (Forbes et al., 1988a,b). Cooling the sample further to 315 K (Figure 8D) resulted in slight narrowing of the sphingosine signals and broadening of the galactose signals, but no changes in chemical shifts were produced. Thus, the cerebroside molecule in the metastable gel preserves the original cerebroside conformation populated in the liquid-crystalline state, although the dynamics of molecules is clearly affected. In contrast, the 318 K spectrum of the sample quenched from 343 to 295 K within 10 min, and relaxed at that temperature for 8 h, was vastly different (Figure 8E) from the analogous one of the metastable phase measured at the same temperature (Figure 8C). The most significant change was splitting of the C1′ signal and shifting its position from 103.7 ppm to 98.5 and 96.5 ppm. Furthermore, the position of the C2 signal was shifted from 53.6 to 48.5 ppm, and the signals of C4 and C5 carbons were also split each into two lines. Further cooling of this sample to 308 and 298 K (Figure 8F,G) produced only greater line widths, but no detectable chemical shift changes. In sharp contrast to NFA-CER, the sample of anhydrous HFA-CER (Figure 8H) displayed a spectrum analogous to that in the liquid-crystalline and metastable states, except for the positions of the carbonyl group and the sphingosine C2 signal.

DISCUSSION

The detailed interpretation of changes of ^{13}C chemical shifts in terms of specific conformations involved can be significantly enhanced by a prior knowledge of shifts for a known conformer as a reference. We first sought to provide such reference by measuring the CP-MAS spectra of the crystalline samples used earlier for X-ray crystallography. Unfortunately, the crystalline sample of the HFA-CER analogous to the one used earlier in the X-ray structural determination (Pascher & Sundell, 1977) was not available. In addition, the ^{13}C CP-MAS NMR spectrum of the authentic crystalline sample of hexamethyl cerebroside (Nyholm et al., 1990) used for X-ray study was very broad, indicating sample aging. Ultimately, we obtained a reference set of ^{13}C chemical shifts by determining the conformation of cerebroside in solution by the analysis of spin−spin coupling

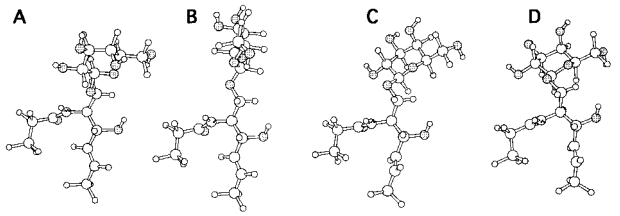

FIGURE 9: Projections of the most stable conformations ($\phi/\psi/\theta_1/\theta_3$) of cerebroside: (A) −sc/ap/−sc/ap; (B) −sc/ap/ap/ap; (C) −sc/−sc/ap/ap with $\psi = -96°$ (C, Nyholm et al., 1990); and (D) −sc/−sc/ap/ap with $\psi = -60°$ (D, Nyholm & Pasher 1993).

constants and NOE values. Chemical shifts in different bilayer phases were then compared with those in solution, and the most prominent changes in chemical shifts of the specific carbon atoms were interpreted in terms of the conformational differences in the vicinity of the ^{13}C probe. Our interpretation is limited to the chemical shift of signals of the anomeric, carbonyl, C2, and hydrocarbon carbons because of the spectral congestion in the range of other carbons.

Conformation of Cerebroside in Solution. The analysis of the coupling constant information indicates that the galactose ring remains in the preferred $^4C_1$ conformation, favored due to the anomeric effect and the conformational preference of the hydroxyl and hydroxymethylene groups in the pyranose system. The NOE data further indicate that the predominant conformation about the C1′−O1 bond is ϕ = −sc, in agreement with the *exo*-anomeric effect (see the next section for discussion). The orientation of the galactose ring with respect to the hydrocarbon chains is hence determined by a combination of three torsional angles affecting bonds between the anomeric carbon and the sphingosine C3 (ψ, θ_1, and θ_3). The more intense H1′−$H1_b$ cross-peak as compared to the H1′−$H1_a$ interaction in the NOESY spectra of both NFA-CER and HFA-CER clearly indicated a smaller distance between the anomeric proton and the upfield $H1_b$, than the downfield $H1_a$ proton. The calculation of the time-averaged H1′−$H1_b$ distance was according to the equation: $r_{H1'-H1b} = r_{H1b-H1a}[NOE_{H1b-H1a}/NOE_{H1'-H1b}]^{1/6}$ (Widmalm et al., 1992), where the determined $NOE_{H1a-H1b} = 0.23$ serves as an internal calibration device, and where the distance between geminal protons $r_{H1a-H1b}$ = 1.73 Å gives a time-averaged distance of $r_{H1'-H1b}$ = 2.1−2.2 Å. This value and the fact that the NOE between H1′ and $H1_a$ was not observed suggest a single −sc/ap conformation about the ϕ and ψ angles, respectively, in agreement with the conformation shown in the X-ray structure data of HFA-CER (Figure 9A) (Pascher & Sundell, 1977; Pascher et al., 1992) and predicted by the MM3 calculations (Nyholm et al., 1993). It is possible that a small amount of the −sc/−sc or −sc/sc conformations is also present, since NOE data are known to exaggerate the amount of conformations with the closest contacts.

Both the vicinal coupling information and the cross-peak intensity in the NOESY spectra indicate that the conformation about C1−C2 (θ_1) is predominantly −sc. The exact calculation of the contribution of +sc and ap rotamers depends on the stereospecific assignment of $H1_a$ and $H1_b$ protons. Without access to cerebroside analogs stereoselectively deuterated at the C1 position, this problem cannot be solved with certainty; however, the available data suggest the assignment of the $H1_b$ proton to the *pro-R* position as

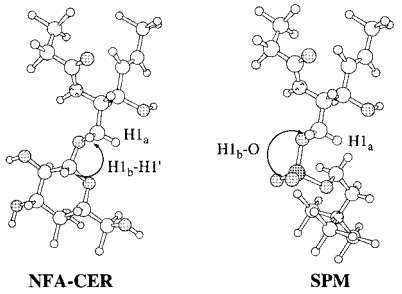

FIGURE 10: Comparison of the predominant conformations of NFA-CER and SPM indicating 1,3-*syn* interaction of H1′ and $H1_b$ in cerebroside, and $H1_b$ and the phosphoryl oxygen atom in SPM.

shown in Figures 1 and 2. This tentative assignment is based on comparison of the chemical shifts and coupling constants of sphingomyelin (SPM; Bruzik, 1988b) and the cerebroside as follows: the positions of the $H1_a$ proton in NFA-CER and HFA-CER are very similar to that of $H1_a$ of sphingomyelin (4.14 ppm and 4.10 ppm in NFA-CER and HFA-CER, respectively, vs 4.11 ppm in SPM), whereas the position of the $H1_b$ proton is strongly shifted downfield in SPM (3.97 ppm in SPM vs 3.60 ppm in NFA-CER and 3.71 ppm in HFA-CER). A similar large chemical shift difference between $H1_a$ and $H1_b$ observed in cerebroside is also typical of more complex sphingolipids (ca. 0.45 ppm; Dabrowski et al., 1988). Further analogies between cerebrosides and SPM include coupling constants $^3J_{H1a-H2}$ (4.8 Hz in NFA-CER, 5.5 Hz in HFA-CER vs 4.6 Hz in SPM) and $^3J_{H1b-H2}$ (3.5 Hz in NFA-CER, 3.3 Hz in HFA-CER vs 3.2 Hz in SPM). These parameters indicate that the θ_1 = −sc conformer is the predominant species (ca. 65%) in both cerebroside and SPM. The conformation of SPM about the C1−O1 bond is mainly ap (Bruzik, 1988b). The only major difference between cerebroside and SPM, the downfield shift of the $H1_b$ proton in SPM, can thus be explained by the field effect brought about by the proximity of the $H1_b$ proton to the P−O dipole of the phosphate group in SPM (Figure 10), as opposed to the anomeric proton in cerebroside. Note that since the phosphate group has three oxygen atoms substituting for other ligands in cerebroside, the apposing arrangement of $H1_b$ and the phosphoryl oxygen would result regardless of any specific conformation about the P−O1 bond. The assignment of the $H1_b$ proton to the *pro-R* position gives rise to a greater contribution of the θ_1 = ap conformation about C1−C2, and virtually eliminates the +sc conformation. The opposite assignment, suggesting the combination of the +sc/ap conformations in the θ_1/θ_3 angles, would result in the unfavorable 1,3-*syn* orientation of the O-1 and O-3 oxygens of sphingosine (Nyholm & Pascher, 1993). The analogous conformations of glycerophospholipids are therefore not populated in solution (Hauser et al., 1988), and were not found in any of the reported X-ray structures of phospholipids (Pascher et al., 1992). The distribution of θ_1 rotamers between −sc and ap, which would require the stereospecific assignment of $H1_a$ as *pro-S* and $H1_b$ as *pro-R*, is thus more consistent with the predominant phospholipid conformations. Overall, the most likely predominant conformation of cerebroside in solution ($\phi/\psi/\theta_1/\theta_3$) is −sc/ap/−sc/ap (Figure 9A), although there is significant contribution from the ψ/θ_1 = ap/ap conformation (Figure 9B), and a smaller one from the ψ/θ_1 = −sc/−sc rotamer (Figure 9C). According to the MM3 calculations, all three conformations are among those with the lowest energy (Nyholm & Pascher,

1993). The −sc/ap/−sc/ap conformation (9A) is featured in the X-ray structure of HFA-CER (Pascher & Sundell, 1977), the −sc/ap/ap/ap conformation is most consistent with the earlier proposed orientation of the hexose residue in the liquid-crystalline bilayers of cerebroside (9B) (Skarjune & Oldfield, 1982), and the −sc/−sc/ap/ap conformation (9C) is consistent with the crystalline state conformation of the permethylated cerebroside (Nyholm et al., 1990).

Conformation of Cerebroside in Bilayers. In view of the large values of conformationally induced changes in ^{13}C chemical shifts (Saito, 1988), the remarkable similarity of these shifts for cerebrosides in the monomer state in solution, and in the aggregated liquid-crystalline state of bilayers, suggests that under both conditions the conformations of cerebrosides are analogous. In fact, more significant differences are observed between the DMSO and methanol solutions: C3 (1.2 ppm), C4 (1.4 ppm), C5 (2.8 ppm), and C1′ (ca. 2 ppm). The extensive similarity of the ^{13}C NMR chemical shift for cerebroside in solution and in liquid-crystalline bilayers strongly suggests that the conformations of both HFA-CER and NFA-CER are analogous in solution and in the liquid-crystalline states, and in the case of HFA-CER also in the metastable gel phase. This similarity can be understood in terms of the relatively weak intermolecular interaction in the two former physical states. Under rapid molecular tumbling in solution, or with fast lateral movement in the liquid-crystalline state, the formation of strong intermolecular complexes, capable of changing conformational equilibria, does not take place, or is quite limited. The rapid quenching of the liquid-crystalline state to the metastable gel state simply traps the predominant conformational species. This conclusion is justified by the fact that the only difference between the spectra of the liquid-crystalline phase and the metastable gel phase is the larger line widths in the latter. The large line widths in the metastable gel phase can be interpreted in terms of slow exchange between conformational isomers, or the existence of frozen rotamers occupying a relatively narrow conformational space. With NFA-CER, the formation of the metastable gel is followed by fast relaxation, so that no spectra of the metastable phase could be obtained with this lipid.

In contrast, large differences were observed between the liquid-crystalline and the gel phase of NFA-CER and between the metastable and stable phases of HFA-CER which are reflective of significant conformational disparities between these states. The most prominent difference between the ^{13}C NMR spectra of the relaxed and metastable gels is in the position of the signal of the anomeric carbon. The available data on the conformational dependence of chemical shifts of the anomeric carbon in glycosides show a strong dependence on the orientation of the glycosidic oxygen atom with respect to a pyranose ring (α- or β-configuration, anomeric effect) (Jarvis, 1994; Kirby, 1983; Lemieux et al., 1979; Bock & Thøgersen, 1982), and on the ϕ angle (*exo*-anomeric effect) (Thøgersen et al., 1982; Houk et al., 1993; Tvaroska & Bleha, 1989). In line with the *exo*-anomeric effect, the ϕ angle is close to −sc in most X-ray crystal structures of carbohydrates (Jeffrey, 1990), and the theoretical calculations also show a high degree of convergence in the ϕ angle among many glycosides (Thøgersen et al., 1982; Bock et al., 1986; Tvaroska & Bleha, 1989). In contrast, the ψ angle is subject to considerable variations which are reflected in significant differences in ^{13}C chemical shifts. For α-glycosides, the existence of the correlation between the ψ angle and ^{13}C NMR chemical shift of the anomeric carbon has been established (Bock et al., 1986; Veregin et al., 1987; Gidley & Bociek, 1988; Durran et al., 1995). In brief, the position of the anomeric carbon signal is shifted upfield as the distance between the anomeric and aglycon protons increases (Bock et al., 1986), or as the ψ angle decreases. For α-glycosides, a decrease in ψ angle by 10° results in a downfield shift of the ^{13}C signal by ca. 2 ppm, and the whole range of conformationally induced shift is ca. 10 ppm (Durran et al., 1995). The ψ vs $\delta_{^{13}C}$ dependence has been used to evaluate conformations of α-cyclodextrins and amyloses (Gidley & Bociek, 1988), and for determination of configurations of alcohols via the corresponding diastereomeric glycosides (Kochetkov, 1984). It was also predicted that an analogous correlation should exist for β-glycosides (Bock et al., 1986), but the paucity of available experimental data precluded verification of this suggestion. The dependence of ^{13}C shifts on the magnitude of the ψ angle originates, most likely, from the so-called γ-effect in NMR (Bierbeck & Saunders, 1976). The 5 ppm upfield shift upon gel phase relaxation is interpreted here as an indication of the reorientation of the galactose ring from the ϕ/ψ = −sc/ap conformation suggested by the study in solution (this work), in the liquid-crystalline state (Skarjune & Oldfield, 1982), and in the crystalline state (Pascher & Sundell, 1977) to −sc/−sc suggested by the X-ray study of permethylated cerebroside (Nyholm et al., 1990). Due to the γ-effect, this conformational change should also cause an upfield shift of the C2 signal, which is in fact observed. It is interesting to note that the position of the anomeric carbon can be shifted downfield as much as to 106.3 ppm in NFA-CER (Figure 7, spectrum C) or upfield to 96.5 ppm in HFA-CER (Figure 7, spectrum E), thus spanning almost the entire expected conformationally-dependent shift range. These extreme values of $\delta_{^{13}C}$ for C1′ most likely represent the pure ψ = ap or ψ = −sc conformers. As explained earlier, it is unlikely that the observed changes in the chemical shift of the C1′ carbon shown in Figures 7 and 8 are due to an inversion of the galactose ring, or a change in the ϕ angle.

It is worthwhile noting, that each stable gel phase of NFA-CER and HFA-CER contains two inequivalent molecules as manifested by the doubling of resonances of the carbonyl group (177.1 and 172 ppm in NFA-CER and 178.4 and 174.1 ppm in HFA-CER), the complex appearance of the C4 and C5 signals, and the doubled signal of C1′ (98.4 and 97.5 ppm in NFA-CER, and 98.4 and 96.5 ppm in HFA-CER). Judging from the ca. 1:1 intensity ratio of resonances in the spectra of NFA-CER, it is possible that the two sets of lines represent individual inequivalent molecules of the dimeric unit in the solid lattice. The fact that in the case of HFA-CER these resonances are not of equal intensity would argue against the molecular complexes of inequivalent molecules, but rather would suggest the coexistence of domains with slightly different packing modes.

Hydrogen Bonding in the Gel Phase and Anhydrous State. It is worthwhile to point out that the ^{13}C CP-MAS spectra of anhydrous samples are consistent with the IR data reported earlier (Bunow & Levin, 1980) indicating that the solid state of NFA-CER is very similar to the hydrated gel phase, and that the solid state of HFA-CER is much different from that of the hydrated gel (presumably metastable). Another IR

study (Lee et al., 1986) indicated the existence of a strong hydrogen bond to the carbonyl group in the stable gel phase of NFA-CER. Our results are in full agreement with these findings. The low-field chemical shift of the carbonyl group of anhydrous HFA-CER at 178.5 and 179.5 ppm (Figure 8H) indicates that this group is involved in hydrogen bonding, while the high-field shift of the C═O group of anhydrous NFA-CER at 172.5 ppm (Figure 7G) indicates the absence of hydrogen bonding.

Hydrocarbon Chain Crystallization. The onset of crystallization, manifested by the appearance of the signal at 32.7 ppm at the expense of the signal at 29.7 ppm, is clear at 330 K, and the whole crystallization process is almost complete at 328 K. These temperatures are 10−15 K lower than the reported temperatures of the main phase transitions (NFA-CER, 345 K; HFA-CER, 341 K) (Curatolo, 1982) obtained from the heating curves. However, since each of the presented spectra was accumulated over several hours, the intensities of the resonances at 32.7 and 29.9 ppm represent most likely a thermodynamic equilibrium between the crystalline and melted phases, although these intensities could be affected by the kinetic phenomena of chain crystallization occurring over the time required for spectra acquisition.

CONCLUSIONS

The results described in this report are significant in three aspects: (i) they indicate that the conformation of cerebroside is not affected by its aggregation into the fluid bilayer assembly, suggesting that the overall conformation is primarily determined by the intrinsic energy of the monomer rather than by intermolecular interactions; (ii) in the solution and liquid-crystalline states, the predominant conformer has the galactose moiety in the $\phi/\psi/\theta_1 = -$sc/ap/−sc conformation, allowing significant mobility of individual molecules and head group hydration; (iii) the transition from the liquid-crystalline phase to the stable gel phase involves most likely reorientation of the galactose residue from the layer-perpendicular to the layer-tilted position via the rotation about C1−O1 (ψ) bond of the sphingosine. These results further underscore the usefulness of ^{13}C CP-MAS NMR in determination of lipid conformations in the aggregated state, and in studies of the mechanism of lipid phase transitions at the molecular level.

ACKNOWLEDGMENT

This work was initiated during the stay of K.S.B. at The Ohio State University. We thank Ming-Daw Tsai of The Ohio State University for his generous support of this work and Irmin Pascher of Göteborg University for review of the manuscript and discussion.

REFERENCES

Barenholz, Y., & Thompson, T. E. (1980) *Biochim. Biophys. Acta 604*, 129−158.

Barenholz, Y., Suurkuusk, J., Mountcastle, D., Thompson, T. E., & Biltonen, R. L. (1976) *Biochemistry 15*, 2441−2447.

Bierbeck, H., & Saunders, J. K. (1976) *Can. J. Chem. 54*, 2985−2995.

Bock, K., & Thøgersen, H. (1982) *Annu. Rep. NMR Spectrosc. 13*, 2−57.

Bock, K., Brignole, A., Sigurskjold, B. W. (1986) *J. Chem. Soc., Perkin Trans 2*, 1711−1713.

Boggs, J. M. (1987) *Biochim. Biophys. Acta 906*, 353−404.

Boyd, B., Magnusson, D., Zhand, Z. Y., & Lingwood, C. A. (1994) *Eur. J. Biochem. 223*, 873−878.

Bruzik, K. S. (1988a) *J. Chem. Soc., Perkin Trans. 1*, 423−431.

Bruzik, K. S. (1988b) *Biochim. Biophys. Acta 939*, 316−326.

Bruzik, K. S., Sobon, B., & Salamonczyk, G. M. (1990) *Biochemistry 29*, 4017−4021.

Bunow, M. R., & Levin, I. W.(1980) *Biophys. J. 32*, 1007−1021.

Curatolo, W. (1982) *Biochemistry* 21, 1761−1764.

Curatolo, W. (1987) *Biochim. Biophys. Acta 906*, 111−136.

Curatolo, W., & Jungalwala, F. B. (1985) *Biochemistry 24*, 6608−6613.

Dabrowski, J., Egge, H., & Hanfland, P. (1980) *Chem. Phys. Lipids 26*, 187−196.

Dabrowski, J., Dabrowski, U., Bermel, W., Kordowic, M., & Hanfland, P. (1988a) *J. Am. Chem. Soc. 110*, 5149−5155.

Dabrowski, J., Trauner, K., Koike, K., & Ogawa, T. (1988b) *Chem. Phys. Lipids 49*, 31−37.

Durran, D. M., Howlin, B. J., Webb, G. A., & Gidley, M. J. (1995) *Carbohydr. Res. 272*, C1−C5.

Estep, T. N., Calhoun, W. I., Barenholz, Y., Biltonen, R. L., Shipley, G. G., & Thompson, T. E. (1980) *Biochemistry 19*, 20−24.

Forbes, J., Husted, C., & Oldfield, E. (1988a) *J. Am. Chem. Soc. 110*, 1059−1065.

Forbes, J., Bowers, J., Shan, X., Moran, L., Oldfield, E., & Moscarello, M. A. (1988b) *J. Chem. Soc., Faraday Trans. 1, 84*, 3821−3849.

Gidley, M. J., & Bociek, S. M. (1988) *J. Am. Chem. Soc. 110*, 3820−3829.

Hakomori, S., & Igarashi, Y. (1995) *J. Biochem. 118*, 1091−1103.

Haas, N. S., & Shipley, G. G. (1995) *Biochim. Biophys. Acta 1240*, 133−141.

Haasnot, C. A. G., De Leew, F. A. A. M., & Altona, C. (1980) *Tetrahedron 36*, 2783−2792.

Harris, P. L., & Thornton, E. R. (1978) *J. Am. Chem. Soc. 100*, 6738−6745.

Hauser, H., Pascher, I., & Sundell, S. (1988) *Biochemistry 27*, 9166−9174.

Houk, K. N., Eksterowicz, J. E., Wu, Y.-D., Fuglesang, C. D., & Mitchell, D. B. (1993) *J. Am. Chem. Soc. 115*, 4170−4177.

Howard, K. P., & Prestegard, J. H. (1995) *J. Am. Chem. Soc. 117*, 5031−5040.

Jarvis, M. C. (1994) *Carbohydr. Res. 259*, 311−318.

Jeffrey, G. A. (1990) *Acta Crystallogr. B46*, 89−103.

Kirby, A. J. (1983) *Relativity and Structure Concepts in Organic Chemistry* Berlin, Springer-Verlag, Berlin.

Klyne, W., & Prelog, V. (1960) *Experientia 16*, 521−523.

Kochetkov, N. K., Chizkov, O. S., & Shashkov, A. S. (1984) *Carbohydr. Res. 133*, 173−185.

Koerner, T. A. W., Cary, L. W., Li, S.-C., & Li, Y.-T. (1979) *J. Biol. Chem. 254*, 2326−2328.

Koynova, R., & Caffrey, M. (1995) *Biochim. Biophys. Acta 1255*, 213−236.

Lee, D. C., Miller, I. R., & Chapman, D. (1986) *Biochim. Biophys. Acta 859*, 266−270.

Lemieux, R. U., Koto, S., & Vorsin, D. (1979*) ACS Symp. Ser. 87*.

Levine, Y. K., Birdsall, N. J. M., Lee, A. G., & Metcalfe, J. C. (1972) *Biochemistry 11*, 1416−1421.

Li, K.-L., Tihal, C. A., Guo, M., & Stark, R. E. (1993) *Biochemistry 32*, 9926−9935.

McCalarney, T., Apostolski, S., Lederman, S., & Latov, N. (1994) *J. Neurosci. Res. 37*, 453−460.

Meulendijks, G. H. W. M., de Haan, J. W., Vos, A. H. J. A., de Ven, L. J. M., & Buck, H. M. (1989) *J. Phys. Chem. 93*, 3806−3809.

Motoki, K., Morita, M., Kobayashi, E., Uchida, T., Akimoto, K., Fukushima, H., & Koezuka, Y. (1995) *Biol. Pharm. Bull. 18*, 1487−1491.

Norberg, P., Nilsson, R., Nyiredy, S., & Liljenberg, C. (1995) *Biochim. Biophys. Acta 1299*, 80−86.

Nyholm, P. G., & Pascher, I. (1993) *Biochemistry 32*, 1225−1234.

Nyholm, P.-G., Samuelsson, B. E., Breimer, M., & Pascher, I. (1989) *J. Mol. Recogn. 2*, 103−113.

Nyholm, P. G., Pascher, I., & Sundell, S. (1990) *Chem. Phys. Lipids 52*, 1−10.

O'Brien, J. S., & Rouser, G. (1964) *J. Lipid Res. 5*, 339−342.
Oldfield, E., Bowers, J. L., & Forbes, J. (1987) *Biochemistry 26*, 6919−6923.
Pascher, I., & Sundell, S. (1977) *Chem. Phys. Lipids 20*, 175−191.
Pascher, I., Lundmark, M., Nyholm, P.-G., & Sundell, S. (1992) *Biochim. Biophys. Acta 1113*, 339−373.
Reed, R. A., & Shipley, G. G. (1987) *Biochim. Biophys. Acta 896*, 153−164.
Rothgeb, T. M., & Oldfield, E. (1981) *J. Biol. Chem. 256*, 6004−6009.
Ruocco, M. J., & Shipley, G. G. (1986) *Biochim. Biophys. Acta 859*, 246−256.
Ruocco, M. J., Atkinson, D., Small, D. M., Skarjune, R. P., Oldfield, E., & Shipley, G. G. (1981) *Biochemistry 20*, 5957−5966.
Saito, H., (1986) *Magn. Reson. Chem. 24*, 835−852.
Sarmientos, F., Schwarzmann, G., & Sandhoff, K. (1985) *Eur. J. Biochem. 146*, 59−64.
Sillerud, L. O., Prestegard, J. H., Yu, R. K., Schafer, D. E., & Konigsberg, W. H. (1978) *Biochemistry 17*, 2619−2628.
Skarjune, R., & Oldfield, E. (1982) *Biochemistry 21*, 3154−3160.
Thøgersen, H., Lemieux, R. U., Bock, K., & Meyer, B. (1982) *Can. J. Chem. 60*, 44−57.
Tkaczuk, P., & Thornton, E. R. (1979) *Biochem. Biophys. Res. Commun. 91*, 1415−1422.
Tvaroska, I., & Bleha, T. (1989) *Adv. Carbohydr. Chem. Biochem. 47*, 45−123.
Veregin, R. P., Fyfe, A. F., Marchessault, R. H., & Taylor, M. G. (1987) *Carbohydr. Res. 160*, 41−56.
Widmalm, G., Byrd, R. A., & Egan, W. (1992) *Carbohydr. Res. 229*, 195−211.
Wynn, C. H., Marsden, A., & Robson, B. (1986) *J. Theor. Biol. 119*, 81−87.
Yoshida, H., Ikeda, K., Achiwa, K., & Hoshino, H. (1995) *Chem. Pharm. Bull. 43*, 594−602.

BI962204R